ISTITUTO NAZIONALE DI FISICA NUCLEARE

Sezione di Milano

INFN/BE-05/01
9 Maggio 2005

RECTANGULAR PULSE FORMATION IN A LASER HARMONIC GENERATION

Simone Cialdi, Fabrizio Castelli, Ilario Boscolo

INFN, Sez. Milano and Dip. Fisica, Univ. Milano, 20133 Milano, Italy

Abstract

In a harmonic generation process the temporal profile of the up-converted pulse undergoes significative changes depending on the input profile and crystal length. A simple theoretical treatment and the corresponding physical view are presented. The matter and the properties of two shaping systems are investigated in view of producing rectangular up-converted pulses as required by laser driven radiofrequency electron sources.

PACS: 42.65.Ky, 42.65.Re

Published by ***SIS–Pubblicazioni***
Laboratori Nazionali di Frascati

1 Introduction

Powerful UV picosecond lasers drive high-brilliance radiofrequency electron sources (rf-gun) [1]. The temporal profile of the laser pulse is required to be of rectangular fashion with fast rise time [1,2]. A rectangular profile is generated inserting in a laser system a shaping device (shaper) which transforms the Gaussian-like profile generated by a laser oscillator into a target one [3]. The pulse length depends on the kind of rf-gun, that is on the operating radiofrequency of the rf-cavities. We refer to the S-band ($\approx\ 3\,GHz$) rf-gun because it is widely used [1]. The laser pulse has to be UV (typically 266 nm), to have a length of 10 ps with a rise time less than 1 ps and an energy of hundreds of microjoules [4]. Lasers suitable to the task are Ti:Saffire and Nd:Glass (and the others of this class) [5] with harmonic generation. The generation of a high energy 266 nm 10 ps rectangular pulse via a third harmonic up-conversion must overcome the problem of the non-linear interaction within a crystal. In fact, the propagation through the crystal produces distortions on the spatial and temporal profiles. The understanding of the profile deformations gives the guidelines for the active setting of the optical components of the shaping system which provides the rectangular pulse profile.

Light pulse manipulation is obtained by amplitude and phase modulation of its spectral components. The two devices most used are the so-called CP-SLM (liquid crystal programmable spatial light modulator) [3] and the DAZZLER (an acousto-optic programmable dispersive filter, also called AOPDF) [6]. The investigation on light pulse shaping was addressed so far to the fundamental harmonic. We extend it to the second harmonic produced by a nonlinear crystal.

In previous papers [4,7] we have investigated two types of shapers for the generation of rectangular target pulses at the first harmonic: one is a CP-SLM shaping system modulating the phases of the spectral components, which is also called 4f-system, see Fig.1(a), and the other is a 4f-2g-system, that is a system which does in succession two operations, the modulation of the amplitude of the spectral components and the temporal stretching of the pulse, see Fig 1(b). The basic operation of a shaping system is to apply a filter function to the input waveform to transform it into a target waveform. In the frequency domain

$$A_o(\omega)\ =\ H(\omega)\cdot A_i(\omega) \tag{1}$$

where A_o, A_i are respectively the output and input waveforms and $H(\omega)$ is the filtering function. The 4f-system has at the center a mask made up of hundreds of pixels where are focused the spectral components and the pixels are patterned as a physical function $M(\omega)$ which does a programmed filter action [4]. The requirement of a rectangular profile of the intensity waveform leaves the degree of freedom of choosing a phase-only filter, that

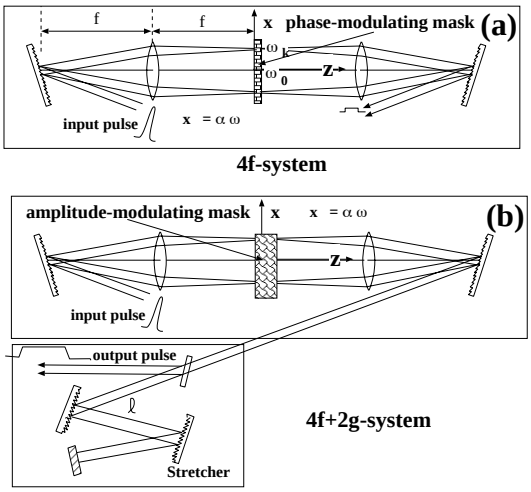

Figure 1: (a) scheme of a 4f-system and (b) scheme of an amplitude-and-chirping-system. The mask at the center of the 4f-system can modulate either the amplitude or the phase of the pulse spectral components. It is set for phase-only modulation when performs a shaping of a laser pulse. The second shaper is composed of two sections: the first modulates the amplitude of the pulse spectral components, the second does the chirp of the components. The amplitude modulation can be accomplished by a 4f-system and the chirp by a pair of gratings, as shown in the figure. The shaping system in this configuration is called 4f-2g-system.

is $H(\omega) = exp[i\,\Phi(\omega)]$. A 4f-system is therefore a phase-only shaper.

A 4f-2g-system (an amplitude-and-chirping-system) has two optical sections: the first is a 4f-system with a mask arranged for amplitude-only modulation $A_o(\omega) = M(\omega)\,A_i(\omega)$, ($M(\omega)$ is a real function) the second section introduces a linear delay time among the spectral components (chirping)

$$\phi(\omega) = \frac{1}{2}\alpha\omega^2. \tag{2}$$

This operation is made up by a pair of gratings, as shown in Fig. 1(b). The output intensity $I_o(t)$ is found by performing the inverse Fourier transform

$$I_o(t) = \left| \int M(\omega) A_i(\omega)\, e^{i\,\frac{\alpha}{2}\omega^2}\, e^{-i\,\omega t}\, d\omega \right|^2 \tag{3}$$

When the output pulse length is much longer [7] than the input pulse length, which means a large α, the integral in Eq. (3) can be written as

$$I_o(t) \approx \{M[\omega(t)]A_i[\omega(t)]\}^2 = \tilde{I}_o[\omega(t)] \tag{4}$$

where $\omega(t) = t/\alpha$. From this Eq. (4) we get that the temporal profile of the pulse $I_o(t)$ is equal to the power spectrum $\tilde{I}_o(\omega)$ profile. We can see that the stretcher simply transfers

the spectral amplitude profile into the temporal amplitude profile. This occurs because a 2g-stretcher establishes a linear relation between frequency and time.

The 4f-system is widely exploited in the pulse shaping technique because it gives a target pulse with phase-only modulation, thus with minimum energy loss. The other shaping system was presented as more suited for generation of rectangular pulses. This conclusion was based mostly on the simpler handling with respect to the former shaper in searching for the right optical configuration [7]. The investigation of the pulse profile evolution in the non-linear interaction in the process of the frequency up-conversion does not change that general consideration. This conclusion holds as long as the laser system has configurational instabilities which require frequent system re-setting for optimized operation.

In this paper we investigate beam propagation and harmonic generation in the common KDP crystal, using a suitable numerical model. Moreover, we analyze and discuss the modification of the pulse profiles, both in time and frequency domain, on the base of a simplified and clarifying analytical theory. We conclude with some considerations about the experimental setup.

2 Beam propagation within a non-linear crystal: the model and the results

For the analysis of the nonlinear interaction leading to second harmonic generation in birefringent χ^2 media, we consider the propagation of quasi-monochromatic electromagnetic fields, with the electric components E_1 at the fundamental angular frequency ω_1 (the ordinary ray in our case), and E_2 at the harmonic frequency $\omega_2 = 2\,\omega_1$ (the extraordinary ray) written as

$$E_i(z,t) = A_i(z,t)\exp\left[i(k_i z - \omega_i t)\right] + c.c\,, \qquad (i=1,2), \tag{5}$$

where A_i are complex amplitudes, k_i are the corresponding wave vectors, z is the propagation axis. We neglect the transverse variation of the fields. In the framework of the slowly varying amplitude approximation, the interaction between co-propagating fields can be described by the coupled differential equations [8]

$$\begin{aligned} \frac{\partial A_1}{\partial z} + \frac{1}{v_{g1}}\frac{\partial A_1}{\partial t} &= i\frac{2\omega_1\, d_{eff}}{c\, n_1}\, A_2\, A_1^*\, e^{i\Delta k\, z} \\ \frac{\partial A_2}{\partial z} + \frac{1}{v_{g2}}\frac{\partial A_2}{\partial t} &= i\frac{\omega_2\, d_{eff}}{c\, n_2}\, A_1^2\, e^{-i\Delta k\, z} \end{aligned} \tag{6}$$

where v_{gi} and n_i are the group velocity and the refraction index relative to the field E_i, d_{eff} is the effective second order susceptibility, and $\Delta k = k_2 - 2\,k_1$ is the phase mismatch.

The proper value of d_{eff} is determined by the angles χ and ϕ defining the propagation direction with respect to the principal optical axis of the selected material. The propagation direction is determined by the condition of maximum interaction efficiency, which corresponds to the condition of perfect phase matching $\Delta k = 0$ [9]. On the other hand, the values of the group velocities and refraction indexes depend on the propagation direction and are calculated by the so-called Sellmeier dispersion equations [10]. In this model we retain the effect of group velocity differences (*i.e.* the temporal walk-off), but neglect the group velocity dispersion, which has effect only for pulse durations well below the ps of our interest [11]. We do not consider, in addition, the effects of higher nonlinearities, which introduce a small phase mismatch and turn out to be relevant only for very energetic short pulses [12,13]. The spatial walk-off due to the small angle between the directions of energy flux and wave vector within the extraordinary ray of birefringent crystals is neglected under the assumption of a broad transverse area of the pulse.

The coupled equations (6) are used to numerically calculate the second harmonic pulse emerging from the non-linear crystal at $z = L$, being L the crystal length. The complex field amplitudes at $z = 0$ are respectively $A_1(0,t)$ for the first harmonic and $A_2(0,t) = 0$ for the second harmonic. $A_1(0,t)$ represents the envelope of the incident pulse at fundamental frequency. It will have a profile suitable for obtaining the target profile after the interaction, and is created by a shaper. A brief description of the numerical method, which has a global second order accuracy, is given in the Appendix. In all the simulations we have selected for definiteness the condition of perfect phase matching $\Delta k = 0$, which guarantees the minimum deformation of the pulses during the interaction.

With the aim of generating a harmonic rectangular pulse of 10 ps, we take into consideration as input pulses for the up-conversion within the non-linear crystal, the two pulses generated by the two shapers of Fig 1. The source laser pulse entering the shapers is assumed to have a Gaussian-like profile with a time FWHM of 100 fs, that is a bandwidth of about 500 GHz. This relatively wide spectral bandwidth is necessary for creating a rectangular laser pulse with fast rise time.

The crystal considered for the harmonic generation is a KDP with a length $L = 500\mu$m, and the maximum intensity of the input signal is chosen below the threshold for damage (which depends on the temporal length of the pulse). The selected length turns out to be a good compromise between the second harmonic conversion efficiency and pulse profile maintenance, as shown by the shape of the output intensity $I_2 = 2\varepsilon_0 n_2^2 v_{g2} |A_2|^2$ of the up-converted pulses for different crystal lengths depicted in Fig. 2. The intensity profile of the second harmonic increases with the crystal length, but the top evolves from the flat to a hilled fashion. A simple theoretical explanation is discussed in the next section.

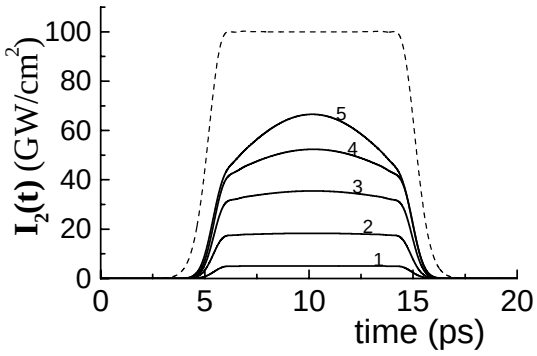

Figure 2: The graphs from 1 to 5 are the harmonic output pulses $I_2(t)$ obtained by Eqs. (6) for crystal lengths spanning the values 200-400-600-800-1000 μm, respectively. The dashed graph is the input signal intensity $I_1(t)$ obtained with the 4f-2g shaping system arranged for that target pulse.

Let us now consider the two shapers.

(1) *Input pulse generated by a 4f-2g shaper*

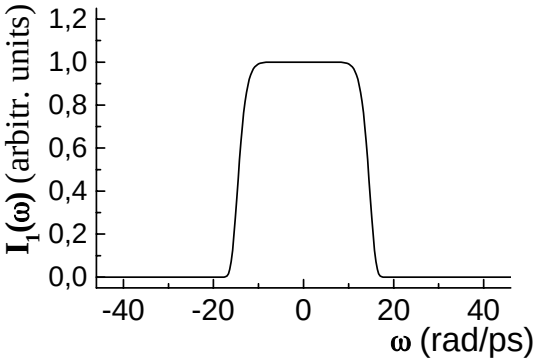

Figure 3: The picture depicts the spectral pulse profile performed by the spectral amplitude modulation. This laser pulse then enters the stretcher (second section of the shaping system) and afterwards enters the non-linear crystal for the second harmonic generation.

We consider first the 4f-2g-shaping system. The amplitude modulation performs a square profile of the pulse power spectrum as depicted in Fig.3. We have run the propagation equations with a set of five input pulses shaped with progressively increased temporal width up to 10 ps. Fig. 4 shows the second harmonic output pulses $I_2(t)$, central column, and the corresponding power spectra $I_2(\omega)$, right column. All the output pulses have the same 10 ps temporal length because the lacking length after the first un-complete stretching (before the SHG, second harmonic generation) is completed by a second stretcher set just after the SHG crystal. The maximum intensity of the input signal profile $I_1(t)$ is selected to obtain near equal values for the intensity maxima of the output pulse, roughly

following the simple rule $I_1(max) \times \sqrt{\Delta t} \approx const$, where Δt is the input pulse FWHM. These pictures show that a rectangular SHG target pulse can be accomplished only with suitable shaping and stretching of the input pulse, before entering the crystal. Moreover, the power spectrum profile in the right column result very similar to the temporal intensity profile for all the input different temporal pulses, in contrast with the behavior of the fundamental harmonic. This fact was discussed in [7], and is theoretically explained in the following section.

(2) *Input pulse generated by a 4f-shaper with phase-only modulation*

We have run Eqs. (6) also with the input pulse obtained by a 4f-system whose mask is arranged for obtaining a 10 ps pulse with phase-only modulation. The appropriate phase function $H(\omega) = exp[i\Phi(\omega)]$ is found by a numerical calculation via an adaptive algorithm. We have followed two different numerical approaches: in one the adaptive algorithm searches for the appropriate phase filter function patterned at the mask pixels which again provides at best the target profile [4]; in the second numerical approach we expanded the phase function in power series

$$\Phi(\omega) = a\,\omega^2 + b\,\omega^4 + c\,\omega^6 + \ldots \tag{7}$$

and the adaptive algorithm searches the coefficients of the series for obtaining an output profile approaching at best the target one.

The output SHG pulses obtained by Eqs. (6) with the two phase functions found along the two lines of calculations are depicted in Fig. 5. The final pulses come out dramatically different in the two cases: the line of the power expansion leads to a fairly smoothed pulse, whereas the line of the direct calculation of the phase of the pixels leads to an output pulse profile flat on the average, but with a lot of superimposed fast spikes.

3 A simplified theory of second harmonic generation with laser pulses with different profiles

In this section we present an approximated theoretical view, which leads to a simplified evolution equation for the second harmonic generated field. This equation allows a picture of the problem which enlightens the physics underlying the observed features of the SHG laser pulses.

Assuming low up-conversion efficiency in crossing the SHG crystal, we can neglect the right hand side in Eq. (6); therefore the slowly varying amplitude of the input pulse A_1 propagate along the crystal remaining practically undepleted. As a straightforward consequence, A_1 can be written as a function depending on the variable $t - z/v_{g1}$ only. The relevant propagation equation for the second harmonic slowly varying amplitude A_2

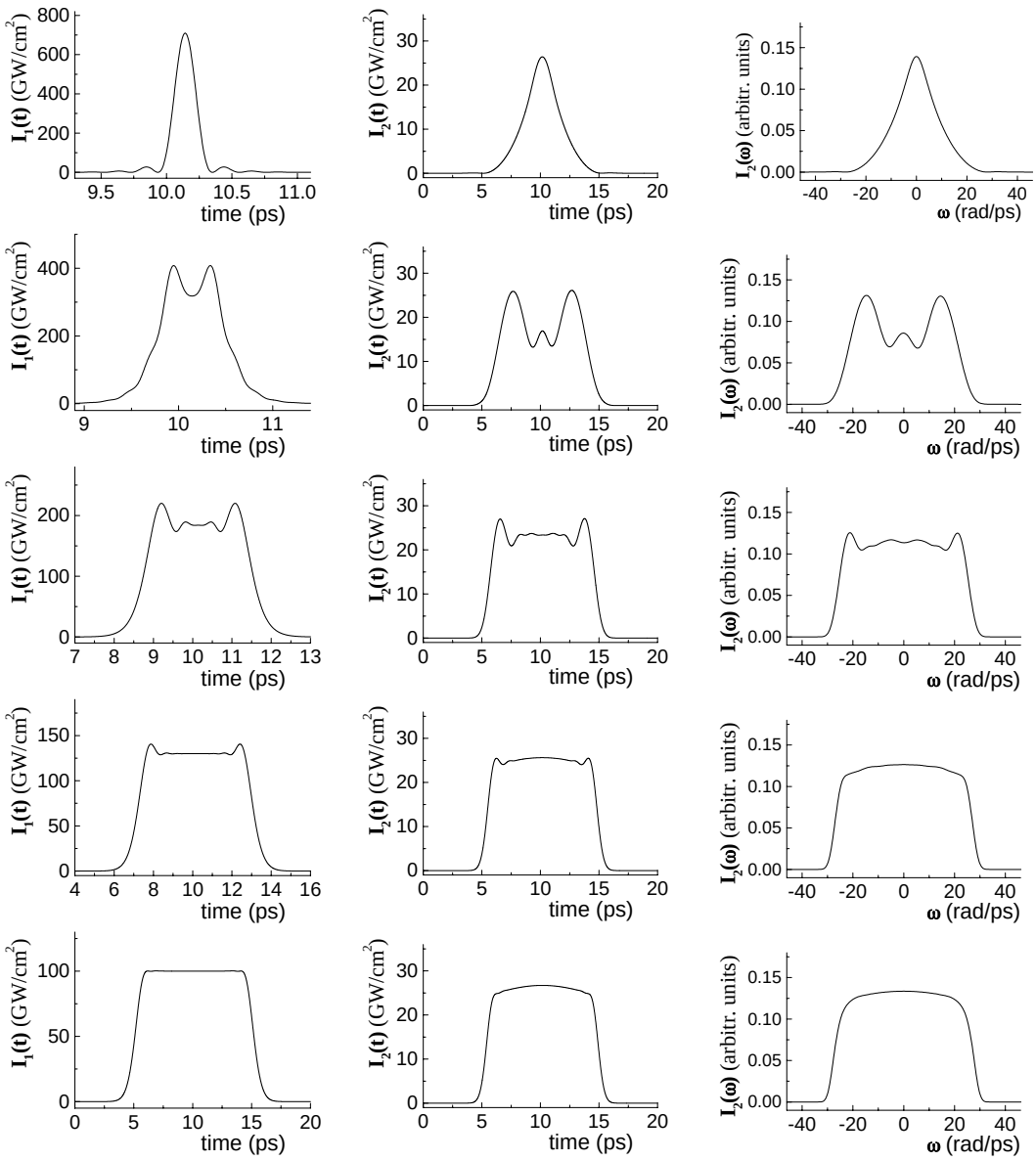

Figure 4: The left column shows the temporal profiles of the input pulses after spectral amplitude modulation and a partial chirping; the center column shows the temporal profiles of the output second harmonic pulses after completing the chirping up to 10 ps length; the right column shows the corresponding normalized power spectra.

now reads

$$\frac{\partial A_2}{\partial z} + \frac{1}{v_{g2}} \frac{\partial A_2}{\partial t} = i\gamma \, [A_1(t - z/v_{g1})]^2 \, e^{-i\Delta k \, z} \, , \tag{8}$$

having put $\omega_2 \, d_{eff}/c \, n_2 = \gamma$. A more useful equation is obtained by changing the time

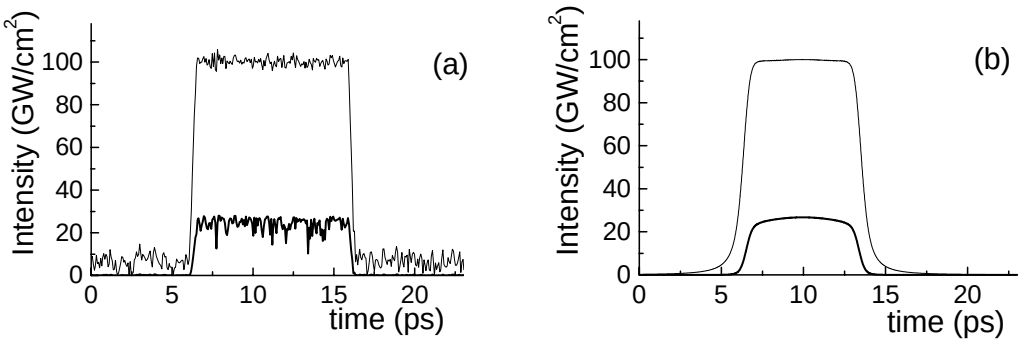

Figure 5: Frame (a): the upper curve is the input signal with a phase-only modulation calculated by an adaptive algorithm directly for the pattern of the mask pixels. The lower curve is the calculated second harmonic output after the interaction within the non-linear crystal. Frame (b): the upper curve is the temporal pulse profile shaped by a phase-only modulation calculated via the optimization of a power expansion coefficients of the phase function by an adaptive algorithm. The lower curve is the up-converted pulse.

frame of reference with $t' = t - z/v_{g2}$

$$\frac{\partial A_2}{\partial z} = i\gamma \left[A_1 \left(t' + \frac{z}{v_{g2}} - \frac{z}{v_{g1}} \right) \right]^2 e^{-i\Delta k z} \equiv i\gamma \left[A_1(t' + \beta z) \right]^2 e^{-i\Delta k z} , \qquad (9)$$

where $\beta = 1/v_{g2} - 1/v_{g1}$ is the group velocity mismatch parameter. In absence of this mismatch (*i.e.* $\beta = 0$) the solution of this equation at the end facet of the crystal is well known [9] and reads

$$A_2(L) = i\,\gamma\, A_1^2\, \frac{e^{-i\,\Delta k\, L} - 1}{-i\,\Delta k} , \qquad (10)$$

showing that $A_2(t) \propto A_1(t)^2$, and the maximum intensity of the second harmonic is obtained when the phase matching condition $\Delta k = 0$ is fulfilled. Assuming the validity of this condition for all the spectral components $\tilde{A}_2(\omega, z)$ of the generated light pulse, we may perform the transformation into the frequency domain of Eq. (9), obtaining

$$\frac{\partial \tilde{A}_2}{\partial z} = i\gamma\, e^{-i\,\beta z \omega}\, \tilde{A}_1(\omega) \otimes \tilde{A}_1(\omega) , \qquad (11)$$

where $\tilde{A}_1(\omega)$ is the incident pulse in the frequency domain, and the symbol $\otimes$ indicates a convolution integral

$$\tilde{A}_1(\omega) \otimes \tilde{A}_1(\omega) = \int \tilde{A}_1(\omega')\, \tilde{A}_1(\omega - \omega')\, d\omega' . \qquad (12)$$

Solving Eq. (11) with zero initial condition, we get the final expression

$$\tilde{A}_2(\omega, z) = i\,\gamma\, z \left(\frac{e^{-i\,\beta z \omega} - 1}{-i\,\beta z \omega} \right) \cdot \tilde{A}_1(\omega) \otimes \tilde{A}_1(\omega) , \qquad (13)$$

This equation (in the frequency domain) indicates that the up-converted pulse is given by the convolution of the input pulse with itself multiplied by a modulation factor.

It is now clear that the non-linear crystal will couple the spectral components of the input pulse at frequencies ω_i and ω_j satisfying the matching condition $\omega_i + \omega_j = \omega_{SHG}$. Therefore the observed intensity $I_2(\omega) \propto |\tilde{A}_2(\omega)|^2$ of the second harmonic will result from the contribution of all the input spectral components complying with the matching condition. The intensity is modulated by a factor $\mathtt{sinc}^2(x)$, where $x = \beta z \omega/2$. This factor defines the frequency bandwidth over which the SHG intensity is significantly different from zero. The bandwidth is progressively reduced with the crystal length as shown in Fig. 6 by the graphs of the quantity $C_N = I_2(\omega)/L^2$ (normalized power spectrum di-

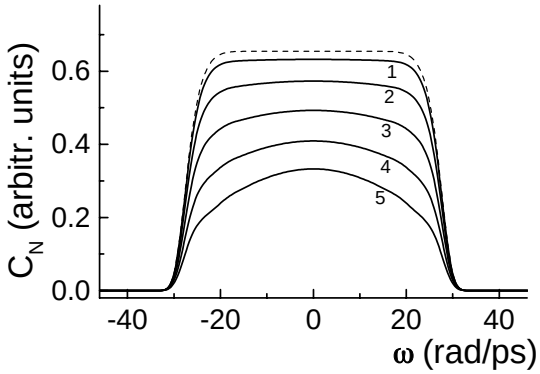

Figure 6: Profiles of the quantity C_N in the frequency domain for a set of different crystal lengths spanning the values 200-400-600-800-1000 μm respectively, as in Fig. 2. The dashed line is the contribution of the convolution term.

vided by length squared) versus the crystal length. The pulse profile evolves from flat to round with the increase of the crystal length L due to the fact that the flat entering pulse is convolved (see the discussion in the next paragraph) with a `sinc` function in the interaction. Note that the spectral content of the output pulse is determined substantially by the `sinc` function bandwidth as the crystal reaches the length of 1000 μm. This effect comes from the higher losses at higher frequencies. This leads to the same rounding effect on the temporal profile, as shown in Fig. 2.

We analyze now the results obtained in the two cases of 4f-2g and 4f-systems on the base of previous considerations, at the fixed crystal length selected for keeping an appropriate frequency bandwidth.

(1) *Input pulse for SHG crystal generated by a 4f-2g shaper*

The pulse to be transformed is assumed to be a transform limited Gaussian pulse. A rectangular spectrum profile $A_1(\omega)$ (as depicted in Fig. 3) is generated by a proper amplitude modulation. When no chirp is applied the expected result of the convolution

integral (12) is simply a simil-triangular shaped SHG pulse. This result is, in fact, obtained by the complete equation system (6) as shown by the first frame second row of Fig. 4.

Let us consider, then, the case with some chirping (that is with the phase modulation $\Phi(\omega) = (1/2)\,\alpha\,\omega^2$). The new amplitude $A_1(\omega)$ will assume the form

$$A_1(\omega) = S_1(\omega)\, e^{i\,\frac{1}{2}\,\alpha\,\omega^2} \tag{14}$$

where $S_1(\omega) = \sqrt{I_1(\omega)}$, with $I_1(\omega)$ the power spectrum of the first harmonic. The amplitude of the second harmonic in the frequency domain will have the expression (discarding the immaterial modulation factor)

$$A_2(\omega) \propto \int S_1(\omega')\, S_1(\omega - \omega')\, e^{i\,\frac{1}{2}\,\alpha[(\omega-\omega')^2+\omega'^2]}\, d\omega'\,. \tag{15}$$

The exponential function

$$e^{i\,\alpha(\frac{1}{2}\omega^2 - \omega\,\omega' + \omega'^2)} \tag{16}$$

is a fast oscillating function for all ω' except at the frequency coordinate $\omega' = \omega/2$; the larger is the coefficient α (that is the longer the stretching), the sooner starts the fast oscillation. Therefore, if α is large enough, the integral turns out to be near zero everywhere except at $\omega' = \omega/2$, *i.e.* that term operates as a δ-function. The integral (15) can be approximately written as

$$\begin{aligned} A_2(\omega) &\approx \int S_1(\omega')S_1(\omega-\omega')\, e^{i\,\alpha(\frac{1}{2}\omega^2 - \omega\,\omega' + \omega'^2)}\, \delta\left(\omega' - \frac{\omega}{2}\right) d\omega' \\ &\approx S_1^2\left(\frac{\omega}{2}\right) e^{i\,\alpha\,(\omega/2)^2} \end{aligned} \tag{17}$$

From this equation we deduce that the spectrum width of the second harmonic is two times larger than that of the first one, and that the spectral profile is similar (squared) to the profile of the first harmonic when the stretching is strong enough. These results reproduces almost exactly those obtained by the simulations with Eqs. (6) as depicted in the right column of Fig. 4. Furthermore, we observe that the delay times of the spectral components for the first and second harmonics are respectively

$$\tau_1(\omega) = \frac{d\Phi_1}{d\omega} = \alpha\,\omega \qquad\qquad \tau_2(\omega) = \frac{d\Phi_2}{d\omega} = \frac{1}{2}\,\alpha\,\omega\,. \tag{18}$$

This result comply with the fact that the temporal width of the second harmonic tends to be the same as the temporal width of the completed stretched first harmonic, as one can see in Fig. 4.

(2) *Input pulse generated by a 4f-shaper with phase-only modulation*

We must consider only the case of the input pulse formed by the phase function obtained by a power expansion. The pulse entering the crystal is already fairly shaped.

From the mathematical point of view we have to treat again with a convolution integral of the type (17), with the exponential phase function even faster oscillating than that considered in the first shaper with a simple chirping. Therefore, the conclusion outlined above is immediate. Incidentally, we could end up straightforward to this conclusion observing that, being the input pulse already formed, we could directly exploit Eq. (10) in the temporal domain.

4 Some experimental considerations

The response function for the generation of a target pulse comes out as numerical solution via an adaptive algorithm. This solution is implemented in the laser system by a proper setting of the shaping system. A computer, running the adaptive algorithm, can drive the system towards the right optical configuration of the shaper, being it inserted in a feedback loop between the output of the harmonic generator and the shaping system. In this configuration the detected output pulse is sent to the computer as input set of data and compared with the target pulse in terms of a cost function [4] and then the shaping system configuration is updated.

However, the operation of the laser system in relation to the pulse profile (provided with the shaper) is very sensitive to mechanical and optical perturbations [4]. Since perturbations (in a large laser system) are un-avoidable, and since a shaping system is capable of bringing off the requested profile counter-reacting to perturbations with a proper re-setting, the laser system must be arranged in an selfcontrolled configuration. The output pulse is continuously measured, sent to a computer for comparison with the target pulse and the computer drives the shaping system to the right spectral amplitude and/or phase re-modulation (depending on the shaping system type): the operational stability implies an adaptive behavior.

In connection with the operation of measuring the output pulse profile and with the operation of computer-assisted setting of the shaping system, we remark that: the detection of a spectrum by a spectrum analyzer is immediate, whereas the detection of a temporal pulse is complicate and difficult. This later operation is customary done by a cross-correlation. In our system the cross-correlation technique cannot be exploited because of the 10 Hz repetition rate. In fact, this low repetition rate leads to a system resetting time of about half an hour. About the technique of the single-shot autocorrelation, we observe that, even if it would be enough fast, for extracting the temporal profile from the autocorrelation graph a numerical de-correlation calculation must be done, and, this calculation needs also a spectrum measurement [15]. These considerations lead to conclude that a 4f-2g shaping system allows an easier handling because a system re-setting is done (i) by

measuring the spectrum of output pulse at each shot and (ii) by connecting the spectrum data to a computer which does the rest (that is compares the output and the target profiles (in our case of 10 ps the profile of the last figure in center column in Fig. 4) and organizes the proper spectral variations).

5 Conclusions

A relatively long and powerful second harmonic laser pulse, efficiently generated trough the interaction within a non-linear crystal, has a rectangular temporal profile only if the profile of the input pulse is properly designed. The production of a proper input pulse requires the implementation in a laser system of a shaping system capable of giving to laser pulses (via spectral amplitude and/or phase modulation) profiles of smooth rectangular-swallow-tailed forms.

Acknowledgments

The work is partly supported by Ministero Istruzione Universita' Ricerca, *Progetti Strategici*, DD 1834, Dec,4,2002 and European Contract RII3-CT-PHI506395CARE.

Appendix

Eqs (6) are conveniently solved with a second order finite difference scheme, appropriate for studies on laser pulse propagation [14]. We first define dimensionless complex amplitudes with

$$C_1 = A_1 e^{-i\Delta k z/2}\sqrt{\frac{2\varepsilon_0 n_1 c}{I_0}}; \qquad C_2 = A_2\sqrt{\frac{2\varepsilon_0 n_2 c}{I_0}} \tag{19}$$

where I_0 is a reference intensity, usually coincident with the maximum of the incident pulse. By changing the independent variables with the relations

$$\tilde{t} = \left(t - \frac{z}{v_{g1}}\right)\left(\frac{1}{v_{g2}} - \frac{1}{v_{g1}}\right)^{-1}; \qquad \tilde{z} = z \tag{20}$$

we get the reduced system of equations

$$\begin{aligned} \frac{\partial C_1}{\partial \tilde{z}} &= i\alpha\, C_2 C_1^* - i\frac{\Delta k}{2} C_1 \\ \frac{\partial C_2}{\partial \tilde{z}} + \frac{\partial C_2}{\partial \tilde{t}} &= i\alpha\, C_1^2 \end{aligned} \tag{21}$$

where

$$\alpha = \omega_1 d_{eff} \sqrt{\frac{2I_0}{\varepsilon_0 c^3 n_2 n_1^2}}\,. \tag{22}$$

The finite difference scheme is obtained by dividing the $\tilde{z} - \tilde{t}$ plane into a grid with spacing $\Delta\tilde{z} = \Delta\tilde{t}$, and making a second order Taylor expansion of $C_1(\tilde{z},\tilde{t}), C_2(\tilde{z},\tilde{t})$ about the grid points (m,n); the second derivatives are calculated by differentiating the Eqs. 21 and substituting a first order difference approximation for the simple derivatives. Therefore we obtain iterative expressions giving the amplitudes at time advanced grid points $C_i(m,n+1)$ as functions of the preceding time and space values $C_i(m-1,n+1), C_i(m,n)$ and $C_i(m-1,n)$. This procedure is numerically stable and has an overall truncation error of order $(\Delta\tilde{t})^2$.

References

[1] M. Ferrario, M. Boscolo, V. Fusco, C. Vaccarezza, C. Roncisvalle, J. B. Rosenzweig and L. Serafini, "Recent advances and novel ideas for high brightness electron beam production based on photo-injectors," In ICFA Workshop "The physics and application of high brightness electron beams" (Chia Laguna, Sardinia, Italy) 1–6 July 2002.

[2] J. Yang, F. Sakai, T. Yanagida, M. Yorozu, Y. Okada, K. Takasago, A. Endo, A. Yada, and M. Washio, J. Appl. Phys. **92,** 1608–1612 (2002).

[3] A. M. Weiner, Rev. Sci. Instrum., **71,** 1929–1960 (2000).

[4] S. Cialdi, I. Boscolo and A. Flacco, J. Opt. Soc. Am. **21**, 1693-1698 (2004).

[5] S. Backus, C. G. Durfee III, M. M. Murname and H. C. Kapteyn, Rev. Sci. Instrum. **69,** 1207–1223 (1998).

[6] F. Verluise, V. Launde, J-P. Huignard, P. Tournois, and A. Migus, J. Opt. Soc. Am. B. **17,** 138-145 (2000).

[7] S. Cialdi and I. Boscolo, Nucl. Insrtrum. Meth. Phys. Res. A 538, 1-7 (2005).

[8] Y.R. Shen, *The Principles of Nonlinear Optics*, Wiley, (New York, 1984)

[9] A. Yariv, *Quantum Electronics*, Wiley, (New York, 1989)

[10] A.V. Smith, SNLO nonlinear optics software, SANDIA National Labs. (http://www.sandia.gov/imrl/X1118/xxtal.htm)

[11] N.C. Kothari and X. Carlotti, J. Opt. Soc. Am. B **5**, 756-764 (1988).

[12] T. Ditmire, A.M. Rubenchik, D. Eimerl and M.D. Perry, J. Opt. Soc. Am. B **13**, 649-655 (1996).

[13] L.D. Noordam, H.J. Bakker, M.P. de Boer and H.B. van Linden van den Heuvel, Opt. Lett. **16**, 971 (1991).

[14] H.Risken and K.Nummedal, J. Appl. Phys. 39, 4662-4672, (1968).

[15] J.W. Nicholson, J. Jasapara, W. Rudolph, F.G. Omenetto and A.J. Taylor, Opt. Lett. **24** 1774-1776 (1999).